ACS OMEGA

Article

Cite This: ACS Omega 2018, 3, 5390−5398

Small Cationic Peptides: Influence of Charge on Their Antimicrobial Activity

José Javier López Cascales,*[,†] Siham Zenak,[‡,#] José García de la Torre,[§] Osvaldo Guy Lezama,[∥] Adriana Garro,[⊥] and Ricardo Daniel Enriz*[,⊥]

[†]Grupo de Bioinformatica y Macromoleculas (BioMac), Area de Química Física, Universidad Politécnica de Cartagena, Aulario II, Campus de Alfonso XIII, 30203 Cartagena, Murcia, Spain

[‡]Laboratoire d'Etude Physique des Matériaux, Département de Physique Energétique, Faculté de Physique, Université des Sciences et de la Technologie d'Oran, BP 1505 El M'Naouer, Oran 31000, Algeria

[§]Facultad de Química, Departamento de Química Física, Universidad de Murcia, Campus de Espinardo, 30100 Espinardo, Murcia, Spain

[∥]INQUINOA (CONICET-UNT) Ayacucho 471, 4000 Tucumán, República Argentina

[⊥]Facultad de Química, Bioquímica y Farmacia, IMIBIO-CONICET, Universidad Nacional de San Luis, Chacabuco 917, 5700 San Luis, Argentina

ABSTRACT: The first stage of the action mechanism of small cationic peptides with antimicrobial activity is ruled by electrostatic interactions between the peptide and the pathogen cell membrane. Thus, an increase in its activity could be expected with an increase in the positive charge on the peptide. By contrast, the opposite behavior has been observed when the charge increases to reach a critical value, beyond which the activity falls. This work studies the perturbation effects in a cell membrane model for two small cationic peptides with similar length and morphology but with different cationic charges. The synthesis and antibacterial activity of the two peptides used in this study are described. The thermodynamic study associated with the insertion of these peptides into the membrane and the perturbing effects on the bilayer structure provide valuable insights into the molecular action mechanism associated with the charge of these small cationic peptides.

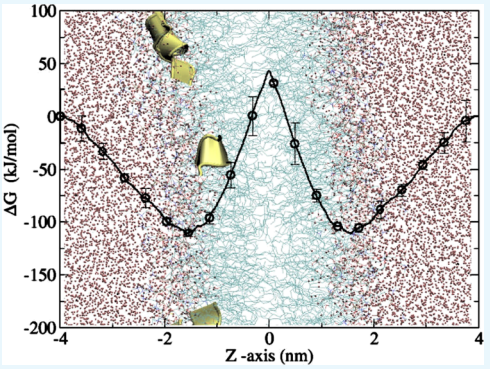

INTRODUCTION

Over many years, antibiotics have proved essential for the therapeutical treatments of different pathogen infections. However, the increase in microbial resistance to antibiotics due to their excessive use during recent decades means that new therapeutical strategies are necessary. In this context, the World Health Organization (WHO) issued a public health warning in 2014, which states that this is not a problem that humanity will have to face in the future but is something that is happening today in the treatment of certain infections resistant to conventional antibiotics. In this context, the increasing incidence of microbial infections resistant to antibiotics is one of the greatest challenges that modern medicine faces today.[1]

In this regard, a great number of cationic peptides that are the first natural barrier against external pathogens have been discovered and characterized. These cationic peptides can be found in mammals, insects, plants, and the skins of some amphibians.[1−10] The two main characteristics of these cationic peptides are that they have positive charges, ranging from +2 to +9, and that they fold in an amphipathic helical conformation, with two well-defined hydrophilic and hydrophobic faces.[1,11,12] Although the alpha conformation is the most common,[13] it has been reported that cationic peptides with β-sheet conformation can also show antibacterial activity.[5,11,14]

The main limitation for developing these cationic peptides as the therapeutic agent is the lack of detailed knowledge about their action mechanism at the molecular level.[15] To help remedy to this situation, our research group has contributed to this topic with two publications. The first one provided insights at the molecular level into the different mechanical properties of binary lipid bilayers of dipalmitoyl phosphatidyl choline (DPPC)/dipalmitoyl phosphatidyl serine (DPPS) in the absence and presence of salt,[16] and the second one suggested an action mechanism for small cationic peptides with antimicrobial and antifungal activity based on a study of the mechanical and thermodynamic properties of binary lipid bilayers of DPPC + DPPS.[17]

In line with the action mechanism of these antimicrobial peptides,[18] there is a wide consensus that these peptides focus their target on the destabilization of the cell membrane of Gram-negative and Gram-positive bacteria and fun-

Received: February 19, 2018
Accepted: April 11, 2018
Published: May 18, 2018

DOI: 10.1021/acsomega.8b00293
ACS Omega 2018, 3, 5390−5398

gus.[1,7,11,14,19,20] Thus, these peptides exert their lytic activity against pathogens by electrostatic interactions with the negative charge of the microbial cell surfaces (favored by the positive charge of these cationic peptides) and subsequent pathogen membrane disruption.[5,7,11,21] Hence, the positive charge of the cationic peptide seems to be a crucial aspect that needs to be considered in the discrimination process between the pathogen and host cells.

In this context, the positive charge of these peptides, together with the amphipathic nature of their alpha helical conformation, seems to be key aspects for their antimicrobial activity.[12,20] However, as reported elsewhere,[14] the number of positive charges of these peptides is a critical parameter in their antimicrobial activity. Generally, an increase in the positive charge enhances the antimicrobial activity of these cationic peptides, although for a number of positive charges above +9 the antimicrobial activity almost disappears.[1,22]

Hence, the development of novel therapeutic agents that could overcome the resistance to standard antibiotics seems to be crucial for continuing the fight against disease. Among novel treatments, small cationic peptides have shown a great potential as a new generation of antibiotics.[1,23] Increased knowledge of the nature and action mechanism of natural cationic peptides has enabled new synthetic peptides to be produced and tested in clinical trials.[24,25] These synthetic peptides (with antimicrobial activity) have shown activity when they were used in animals as models of infections by a variety of pathogens.[12,23,26] However, despite the great expectations in this field, clinical trials have been limited, and none has been approved for use in humans to date. Instead, trials have been limited to topical applications[26] because peptides that apparently have negligible lethality and toxicity for mammalian cells in vitro have frequently been found to be toxic when they were injected into the bloodstream.[25] Another important aspect related to this delay in the use of such peptides in clinical trials is their high cost of manufacture and, hence, of prescription drugs.[27] To overcome all the inconveniences associated with the use of these cationic peptides as new antibiotics, new short-chain peptides, which have less than 12 residues and are cheaper to manufacture, have been synthesized as candidates for use in clinical trials. Our research group has previously reported new small peptides (sequences possessing 11 and 12 amino acids) with significant antibacterial activity.[28] More recently, we reported on a peptide with nine amino acids (Arg-Gln-Ile-Arg-Arg-Ile-Ile-Gln-Arg-NH_2) that had a strong antibacterial effect against a panel of pathogenic bacteria;[29] in fact, this compound is the smallest peptide with the strongest antibacterial activity reported to date.

The molecular dynamics (MD) simulation technique has been accepted as a valuable complementary tool in experimental studies to understand complex systems. In this work, we focus on studying the effect of these cationic peptides on the structure of a cell membrane model to predict their antimicrobial activity. With this goal, a detailed study was carried out with two small cationic peptides, *RQWRRWWQR-NH_2* and *RKFRRKFKK-NH_2* with charges +4 and +7, respectively, which are henceforth called pep+4 and pep+7, in which the N-terminal amines were not considered for the charge of these peptides. In the first step, the two peptides were synthesized, and their antimicrobial activity was tested. In the second step, the activity of these peptides was associated with the level of perturbation of a phospholipid bilayer of DPPC in the presence of different concentrations of the peptide adsorbed on its surface. The reason why a zwitterionic membrane was chosen as the cell membrane model instead of a negatively charged one (which could be associated with a pathogen cell membrane) is that (as was described recently in the dynamic action mechanism of antimicrobial peptides[17]) the activity of these peptides arises from the induction of phospholipid domains in the pathogen membrane, and the subsequent insertion of the peptides into the rich domains of zwitterionic phospholipids, when the peptide reaches a certain concentration on the outer cell membrane.

This work also studies the thermodynamic process associated with insertion of the peptide into the membrane and how the architecture of the cell membrane is perturbed in the presence of cationic peptides of different charges.

RESULTS

Antibacterial Activity. Two peptides were chosen, whose structural characteristics it was thought, would give different activities and allow their molecular behavior to be evaluated when they interact with the biological membrane.

We previously reported that pep+4 possesses a significant antifungal activity against *Candida albicans* and *Cryptococcus neoformans*,[30] whereas pep+7 does not have any effect in this respect.[31] However, the antibacterial activity of both peptides has not been evaluated to date. It should be noted that in both cases, amphipathic α-helical conformation has been reported to be the most favorable. Thus, in the first step of the study, and as a preliminary analysis, the Edmundson wheels obtained for these two peptides were evaluated (see Figure 1). From this

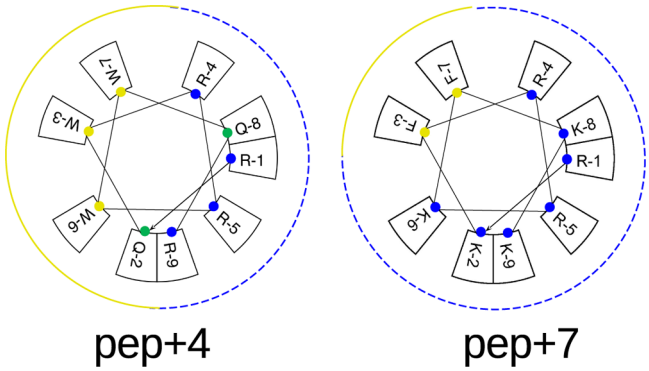

Figure 1. Edmundson representation obtained for the two peptides, pep+4 and pep+7.

figure, it is evident that pep+4 has two perfect differentiated faces of a similar size: a cationic face (marked with blue cut lines) and a most hydrophobic face (represented by solid yellow lines). The first face identifies residues R4, Q8, R1, R5, and R9, accounting for the mutual Coulombic binding. These residues are located on the same side of the helical peptide, which was therefore designated the charged face. These positively charged residues are able to interact with the hydrophilic part of the lipids. The noncharged face is formed by three hydrophobic (W6, W3, and W7) residues and one polar (Q2) residue. This type of distribution has been proposed as an essential structural characteristic for this type of peptide to present antibacterial[28] and antifungal[31] activity. By contrast, pep +7 (Figure 1) has a large cationic face covering most of the Edmundson representation where all the cationic residues are concentrated (R4, K8, R1, R5, K9, K2, and K6) and only a

DOI: 10.1021/acsomega.8b00293
ACS Omega 2018, 3, 5390−5398

small hydrophobic portion formed by F3 and F7. This is a striking difference with respect to pep+4.

To make a more accurate evaluation of the differential structural characteristics of these two peptides, in a second stage of the study an electronic analysis of these compounds was performed by analyzing their molecular electrostatic potentials (MEPs).[32] Molecular electrostatic fields and MEPs provide a relevant description of the capacity of peptides to generate stereoelectrostatic forces. More positive potentials reflect nucleus predominance, while less positive values represent rearrangements of electronic charges and lone pair of electrons. The MEPs of peptides pep+4 and pep+7 are shown in Figure 2. To better appreciate the electronic behavior

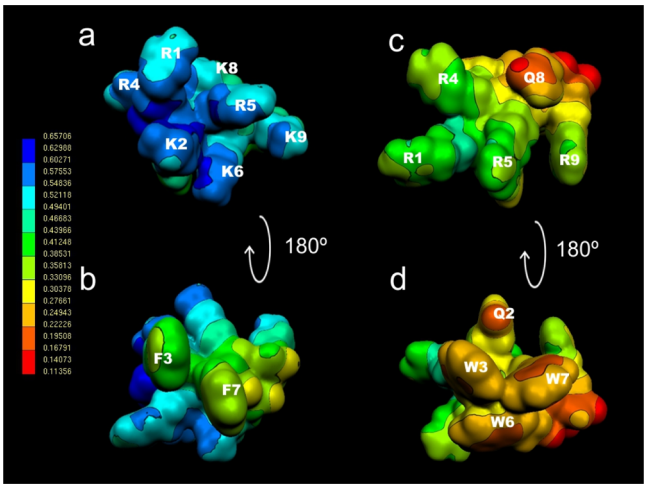

Figure 2. Electrostatic potential-encoded electron density surfaces of the structures of peptides pep+4 (c,d) and pep+7 (a,b). The coloring represents electrostatic potential with red indicating the strongest attraction to a positive point charge and blue indicating the strongest repulsion. The electrostatic potential is the energy of interaction of the positive point charge with the nuclei and electrons of a molecule. It provides a representative measure of overall molecular charge distribution.

of pep+4 and considering that two different faces were signaled in Figure 1, we present the MEPs of pep+4 and pep+7, showing the two faces. Figure 2a shows the charged face of pep+7, which is characterized by the presence of seven cationic residues (R-1, K-8, R-5, K-9, K-6, K-2, and R-4). It is clear from the figure that blue color shows the extended moiety of pep+7. In turn, Figure 2b shows the small portion of the hydrophobic zone of pep+7 characterized by only two residues, F-3 and F7.

As expected, significant differences can be seen in the electronic distributions of pep+4 with respect to pep+7 (compare Figure 2a,b with 2c,d). Pep+4 shows two well-differentiated but similar-sized portions. Its cationic face is characterized by the four cationic residues (R4, R1, R5, and R9) and one polar residue (Q8), while the hydrophobic face is formed by three hydrophobic amino acids (W6, W3, and W7) and one polar residue (Q2). It has been previously reported that peptide and lipid association occurs through the formation of salt bridges between the positively charged residues and the lipid phosphate groups.[33] In addition, tryptophan fluorescence studies have previously shown the importance of positively charged residues for the initial binding of these small peptides to negatively charged vesicles because double R/K/A mutations significantly decreased the binding affinity.[34] The MEPs of pep +4 suggest that the above-mentioned residues (R1, R4, R5, and R9) could be responsible for the initial binding in pep+4.

It has been reported that the mutation of strategically located tryptophan residues decreases internalization, whereas double substitution completely inhibits peptide internalization.[35−37] It appears that charge neutralization is required for the peptide to insert itself deeply into the hydrophobic core of the membrane. A significant hydrophobic face appears to be important in this sense. On the basis of our results, it is reasonable to expect that pep+4 could present antibacterial activity because, despite its small size, it meets the previously established structural requirements for the active peptides. In contrast, pep+7 should not possess any antibacterial effect. After obtaining the stereoelectronic characteristic of the two peptides, our next step was to evaluate their antibacterial activity. As expected, pep +4 showed a significant antibacterial activity against a panel of pathogenic bacteria, whereas pep+7 had no antibacterial effect. In the next sections, we present and discuss the results of extensive MD simulations to explain at the molecular level the influence of charge on the antibacterial activity of these small peptides.

Peptide Distribution. Figure 3 shows the peptide distribution function for both types of peptides studied in

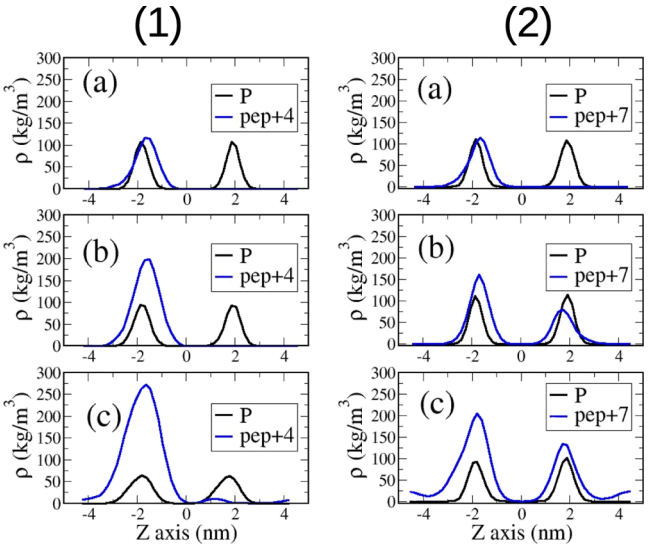

Figure 3. Peptide and DPPC phosphorous (P) distribution after 100 ns of simulation time. Left column corresponds to pep+4 and right column to pep+7. Labels (a−c) refer to peptide/phospholipid ratios of 1/32, 1/16, and 1/8, respectively.

this work, corresponding to pep+4 and pep+7, after 100 ns of simulation time. In both figures, it can be seen how pep+4 is distributed on both leaflets of the bilayer, even though both peptides were placed near the same leaflet, as can be seen in Figure 4.

Figure 3 shows that the peptide concentration of pep+4 adsorbed on the membrane increases almost linearly with the number of peptides added to the system. This behavior permits a certain peptide threshold concentration to be reached on the membrane surface that is sufficient to induce the disruption of the bilayer structure, as was discussed elsewhere.[17] By contrast, an increase in the pep+7 concentration is not reflected in an increase in the peptide concentration on the surface, making it almost impossible to reach a threshold concentration that can perturb the membrane structure, that is, to show antimicrobial

DOI: 10.1021/acsomega.8b00293
ACS Omega 2018, 3, 5390−5398

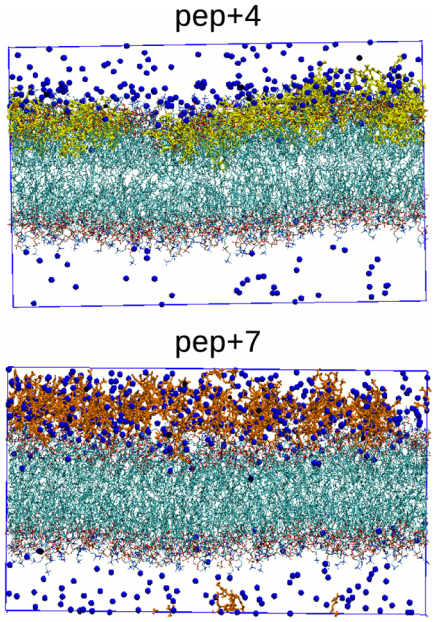

Figure 4. Snapshot of the starting configuration of DPPC bilayers in the presence of the two peptides studied in this work. In both cases, the peptides were placed near one leaflet of the lipid bilayer. (Up) DPPC in the presence of 40 pep+4 (yellow) and (down) DPPC in the presence of 40 pep+7 (red). Blue beads correspond to chloride ions used to balance the total charge existing in the system. Water has been removed for clarity.

activity. The migration of pep+7 in Figure 3 from one leaflet to the other is clearly associated with the electrostatic repulsions between neighboring peptides because of a poor charge screening between them, as a consequence of their low ability to penetrate into the bilayer compared with the behavior shown by pep+4. We remark that this migration of pep+7 from one side to the other of the lipid bilayer takes place through the water layer associated with the periodicity of the computational box and never across the lipid bilayer.

Order Parameter, S_{CD}, and Surface Area per Lipid Molecule. The order parameter, S_{CD}, provides information about the disorder in the hydrocarbon region inside the lipid bilayer, a property that can be determined experimentally from ^{2}H NMR splittings. Thus, from the values of quadrupolar splittings, $\Delta\nu_Q$, obtained from ^{2}H NMR, the deuterium order parameter, S_{CD}, can be calculated as follows

$$\Delta\nu_Q = \frac{3C\langle S_{CD}\rangle}{2} \quad (1)$$

where C is the quadrupole coupling constant (C = 170 kHz[38]) and S_{CD} is the order parameter of a given C−D bond. Furthermore, the order parameter can be extracted directly from simulations using

$$\langle S_{CD}\rangle = \frac{\langle 3\cos^2\phi - 1\rangle}{2} \quad (2)$$

Here, ϕ is the angle between the C−D bond and the bilayer normal and the average is obtained over the simulation time and the number of identical molecules in the computational box. However, bearing in mind that hydrogens from methylene groups are not explicitly considered in DPPC in our simulations, the order parameter corresponding to a given C−D bond can be calculated using a methodology described elsewhere.[39]

Figure 5 shows how the presence of pep+7 does not perturb the hydrocarbon structure in the interior of the phospholipid bilayer throughout the range of concentrations studied in this work. This behavior contrasts with that measured in the presence of pep+4, in which, for a given peptide concentration above a threshold value, a noticeable increase in the phospholipid disorder is measured as the peptide concentration increases.

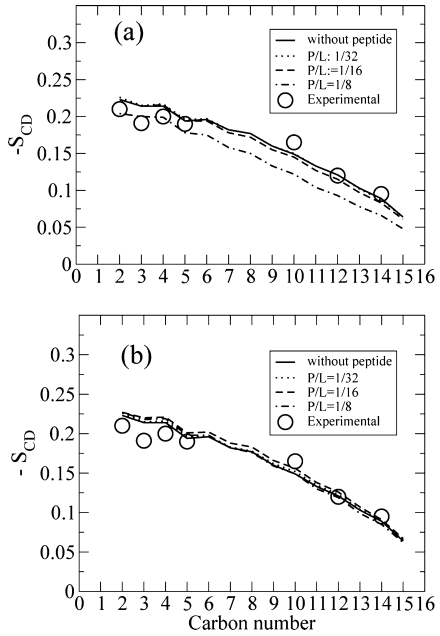

Figure 5. Simulated deuterium order parameters—S_{CD} along the DPPC hydrocarbon tail of a DPPC bilayer, for different peptide/phospholipid ratios, (a) pep+4 and (b) pep+7. Circles correspond to the experimental data of a DPPC bilayer in the absence of peptides at 350 K.[40]

Furthermore, Table 1 shows the surface area per lipid molecule for different peptide/lipid ratios in our simulations and also shows how the presence of pep+7 produces a shrinkage in the surface area per phospholipid with respect to its value in the absence of peptides in solution. This result contrasts with those obtained in the presence of pep+4, in which the lipid surface was seen to expand. These results closely agree with the results obtained from the deuterium order parameter (see Figure 5), in which an increase in the disorder of the hydrocarbon region with the P/L ratio was measured, which was associated with an increase in the free space between adjacent phospholipids, as it would be expected from an increase in the surface area per lipid molecule.

Thickness of the Lipid Bilayer. To estimate the effect of the presence of cationic peptides on the thickness of the lipid bilayer, Figure 6 depicts the phosphorus distribution on both lipid leaflets that form the lipid bilayer, in the presence and absence of cationic peptides.

Figure 6 shows how the presence of pep+7 was no affected on the thickness of the lipid bilayer at any concentration. This result contrasts with those obtained for pep+4, where for a given threshold concentration a reduction of 20% in the thickness of the lipid bilayer was evident.

DOI: 10.1021/acsomega.8b00293
ACS Omega 2018, 3, 5390−5398

Table 1. Surface Area of DPPC for Different Peptide/Phospholipid Ratios of Peptides Adsorbed on the Lipid Bilayer

	peptide/DPPC ratio			
peptide	without peptides	1/32	1/16	1/8
pep+7	0.698 ± 0.004	0.664 ± 0.005	0.659 ± 0.004	0.672 ± 0.005
pep+4	0.698 ± 0.004	0.673 ± 0.003	0.682 ± 0.003	0.719 ± 0.006

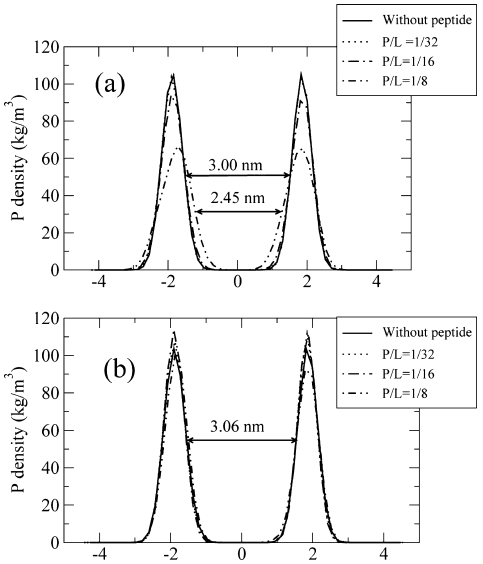

Figure 6. Phosphorous distribution across the lipid bilayer for different peptide/phospholipid ratios in the presence of pep+4 (a) and pep+7 (b).

Bending Modulus, k^b, of the Lipid Bilayer. The bending modulus, k^b, is calculated as follows

$$k^b = \frac{K_A \xi^2}{24} \tag{3}$$

where K_A corresponds to the compressibility modulus of the membrane and ξ the effective thickness of the lipid bilayer, calculated as $\xi = d_{P-P} - 1$, where d_{P-P} is the distance between the maximum of phosphorus distribution of both lipid leaflets that form the lipid bilayer. K_A is calculated as follows

$$K_A = \frac{k_B T A}{\sigma^2(A)} \tag{4}$$

where k_B is the Boltzmann constant, T the temperature, A the surface area per lipid molecule, and $\sigma^2(A)$ the mean square fluctuation of the interfacial area.

Table 2 shows the bending modulus of the different systems studied in this work. In the absence of peptides, a k^b value of 29 k_BT was measured for the lipid DPPC bilayer. This value agrees with the experimental data obtained from pipette aspiration[41,42] and neutron spin echo[43] measurements, which gave values of k^b in a range of 11−30 k_BT, depending on the length of the lipid hydrocarbon tails and temperature.

Table 2. Bending Modulus, k^b, of the DPPC Bilayers for Different Peptide/phospholipid Ratios[a]

	$k^b/(k_BT)$			
	peptide/lipid ratio			
peptide	without peptides	1/32	1/16	1/8
Pep-7	29	28.3	32	30
Pep-4	29	36	48	22

[a] k_B corresponds to the Boltzmann constant and T the temperature.

In the presence of pep+7, k^b remains almost unaltered over the whole range of concentrations studied as a consequence of the poor interactions between the peptides and the lipid bilayer, as discussed above. By contrast, in the presence of pep+4, k^b increased as the number of peptides adsorbed on the surface of the lipid bilayer increased as well, until a given threshold concentration was reached, corresponding to a peptide/lipid ratio of 1/8, when k^b is 25% lower than that of the value of the lipid bilayer in the absence of peptides. This sharp decrease in the bending modulus of the lipid bilayer (i.e., an increase in its flexibility) gives an idea of how the mechanical properties of the lipid membrane are disrupted, as a prelude of the lytic activity of these cationic peptides.

Lateral Pressure, $\pi(z)$. The lateral pressure profile across a lipid bilayer, $\pi(z)$, is a key aspect related with its mechanical stability. Computationally, the lateral pressure profile can be estimated using the algorithm of Lindhal and Edholm,[44] where a detailed description of how this property is calculated can be found elsewhere.[17]

In this regard, Figure 7 shows the lateral pressure profile, $\pi(z)$, for the DPPC bilayer in the absence and presence of peptides adsorbed on the membrane.

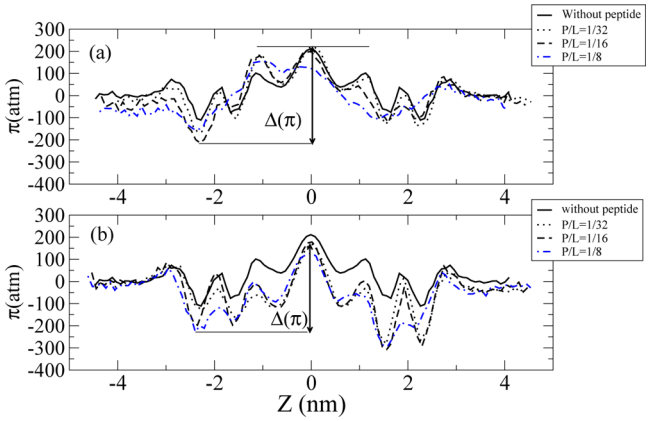

Figure 7. Lateral pressure $\pi(z)$ of the DPPC bilayer in the absence and presence of peptides for different peptide/phospholipid ratios. (a) Corresponds to pep+4 and (b) to pep+7.

Unfortunately, there is not an experimental verification of this property, although the results obtained in our simulations are in a reasonable agreement with the results provided by Kamo et al.[45] from fluorescence measurements, in which a lateral pressure of 350 atm was estimated in the middle of a lipid bilayer.

Figure 7 shows how the pressure profile is not perturbed by the presence of pep+7 in comparison with the case in which pep+4 is present, showing the existence of a threshold concentration from which a noticeable perturbation of the bilayer stability takes place. In this regard, and on the basis that an increase in the pressure is associated with an increase in the

DOI: 10.1021/acsomega.8b00293
ACS Omega 2018, 3, 5390−5398

instability of the bilayer architecture, this behavior is in good agreement with the higher antimicrobial activity of pep+4 than pep+7, in spite of its high positive charge. However, in both cases, the main perturbation takes place in the vicinity of the phospholipid/water interface, in line with the discussion described above.

Thermodynamic Study of Peptide Insertion in the Lipid Bilayer. *Free Energy Associated with Peptide Insertion into the Lipid Bilayer.* The partition function of a certain species between two mediums is directly related with the difference of free energy associated with this process, as follows

$$\Delta G(z) = -RT \ln \frac{C(z)}{C^*} \tag{5}$$

where $C(z)$ corresponds to the species concentration at a certain position z perpendicular to the interface and C* its concentration in the bulk solution. To estimate the potential mean force (PMF) associated with the insertion of peptides into a lipid bilayer, two peptides were considered simultaneously in our simulations, and the Umbrella[46] and WHAM[47] were the computational methods used to estimate the PMF. Thus, we placed one of the two peptides in bulk water and the other in the middle of the lipid bilayer formed by 288 DPPC (144 DPPC per leaflet) and 17 516 water molecules with their corresponding Cl^- to balance the charges of the system. Hence, starting from this first conformation, peptides were displaced along the *Z*-axis to estimate the PMF across the lipid bilayer.[17]

Figure 8 shows $\Delta G(z)$ corresponding to the insertion into the DPPC bilayer of the two cationic peptides studied in this work. From Figure 8, it can be seen how the adsorption of peptides into a lipid bilayer is a spontaneous process for both peptides, which corresponds to the negative values of $\Delta G(z)$. However, this process is −37 kJ/mol lower for pep+7 than for pep+4, as a consequence of the strong electrostatic interactions between peptide/lipid bilayers. On the other hand, a thermodynamic barrier to the insertion of these peptides into the bilayer emerged, which is 39 kJ/mol higher for pep+7 than for pep+4. This difference may be associated with the existence of tryptophan residues in pep+4 but not in pep+7, and hence, its insertion into the hydrocarbon region of the lipid bilayer is favored. Hence, from this thermodynamic study, we conclude that the insertion of pep+4 into the core of the hydrocarbon region of the lipid bilayer is easier than it is for pep+7, which could explain its antibacterial activity. For its part, pep+7 cannot penetrate into the membrane to disrupt the membrane structure and hence perturbs the mechanical properties of the lipid membrane to provide lytic activity, remaining anchored to the surface of the lipid bilayer.

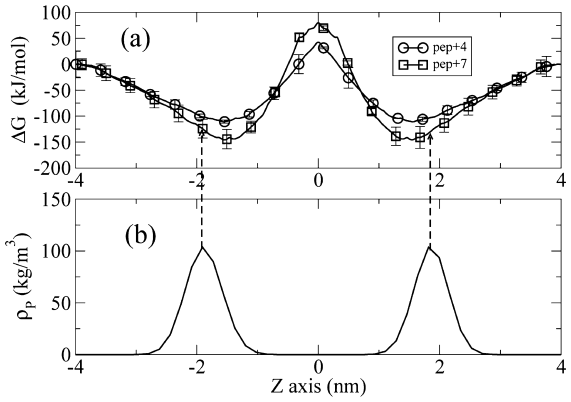

Figure 8. (a) Free-energy profile associated with the insertion of cationic peptides into a DPPC bilayer. (b) Atomic phosphorous distribution across the DPPC bilayer.

Enthalpy and Entropy of the Peptide Insertion. Obtaining thermodynamic information related to peptide insertion into the lipid bilayer is of crucial importance in order to understand the thermodynamic driving force that rules the interaction of these small cationic peptides with a lipid membrane.

In this regard, from classical thermodynamics, it is known that entropy ΔS, enthalpy ΔH, and the free energy ΔG are related by the well-known expression

$$\Delta G = \Delta H - T\Delta S \tag{6}$$

where ΔH and ΔS correspond to the variation of enthalpy (energy) and entropy (disorder) involved with this thermodynamic process.

According to classical thermodynamics, the variation of entropy associated with a given thermodynamic process can be calculated from the variation in free energy at two different temperatures, as follows

$$\left(\frac{d\Delta G}{dT}\right)_P = -\Delta S \tag{7}$$

A solution to this differential equation can be approximated numerically as follows

$$-\Delta S = \left(\frac{d\Delta G}{dT}\right)_P \simeq \frac{1}{2\Delta T}(\Delta G(T+\Delta T) - \Delta G(T-\Delta T)) \tag{8}$$

Thus, from the free-energy profile of ΔG at two different temperatures, the entropy of peptide insertion into a phospholipid bilayer can be estimated. Once ΔS has been calculated, the enthalpic contribution to the free energy can also be estimated, using eq 6. In our case, two additional profiles of free energy corresponding to 340 and 360 K were obtained. Figure 9 shows the free energy (ΔG), enthalpy (ΔH), and entropy (ΔS) profiles associated with the insertion of pep +4 and pep+7 to the lipid bilayer at 350 K.

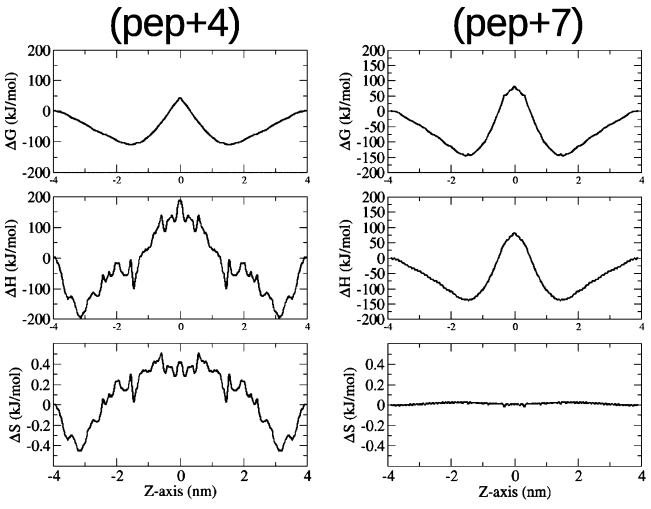

Figure 9. ΔG, ΔH, and ΔS associated with the insertion of pep+4 and pep+7 into a DPPC bilayer.

DOI: 10.1021/acsomega.8b00293
ACS Omega 2018, 3, 5390−5398

With regard to pep+4, we observe how ΔH is negative (exothermic process) in the vicinity of the lipid/water interface with a value of −194 kJ/mol (or −46.4 kcal/mol) and becomes positive (endothermic) in the middle of the lipid bilayer, with a value of 189 kJ/mol (or 45 kcal/mol). The binding enthalpy of pep+4 to the lipid bilayer is a reasonable good agreement with the values of −14.4 and −17.0 kcal/mol measured by isothermal titration calorimetry of pexiganan[48] and magainin-2 bound to vesicles,[26,48,49] once the difference in size and charge between these species has been discounted. With regard to the variation of entropy, there was a decrease at the vicinity of the bilayer/water interface (as expected for strong electrostatic interactions with the polar head of lipids at the lipid/water interface), followed by an increase toward the aliphatic region inside the bilayer. Thus, from the analysis of ΔH and ΔS, it is concluded that insertion into the lipid bilayer is governed by an increase in the entropic contribution to the free energy inside of the lipid bilayer.

In the case of pep+7, ΔH presents a minimum of −139 kJ/mol in the vicinity of the lipid bilayer (or −33 kcal/mol), a value that is also in reasonable agreement with the values of ΔH for pexiganan and magainin-2 bound to vesicles, as mentioned above. It is important to note that unlike pep+4, ΔH follows the same trend as ΔG, as a consequence of the almost null contribution of the entropy to the free energy. This means that the free energy is mainly dominated by its energetic term, ΔH, while the contribution of the entropy to the free energy is very low. This low contribution of the entropy is associated with the strong electrostatic interactions between the peptides and the polar heads of phospholipids, which dramatically reduces the mobility of these peptides at the bilayer/solution interface, in perfect agreement with the results obtained by simulation.

This interpretation is based on the results concerning the disorder of lipid bilayers in the presence of peptides. Thus, in the presence of pep+4, a decrease in the order parameters (an increase in the disorder in the hydrocarbon region of the lipids) of phospholipids was measured, unlike in the case of pep+7, in which the order parameters of the phospholipids remained constant over the whole range of peptide concentrations studied in this work.

From the analysis and comparison of ΔG, ΔH, and ΔS for both peptides, we conclude that an excess of charge reduces the disorder inside the lipid bilayer associated with the presence of these peptides, that is, the possibility of disrupting the lipid bilayer structure decreases. Hence, the results suggest that entropy is the key property that must be investigated to predict the antimicrobial activity of these small cationic peptides.

CONCLUSIONS

There are many theoretical and experimental studies that have focused on the influence of charge on the antibacterial activity of these small peptides. In this sense, it is known that to achieve a certain level of antimicrobial activity, the charge of these cationic peptides must be between +2 and +9 (depending on the size of the peptide). The results presented in this work are the first to provide an explanation (at the molecular level) of why charged peptides are not able to reach the threshold concentration necessary to produce the deformation of the membrane, that is, its subsequent biological activity.

To increase our knowledge of the role played by the charge in the antimicrobial activity of new synthetic peptides, two peptides with charges +4 and +7 were studied. From in vitro studies, it was demonstrated how the peptide with charge +7 does not show antimicrobial activity, whereas the peptides with charge +4 do.

From the thermodynamic study of peptide insertion into a phospholipid bilayer of DPPC, and evaluation of the bilayer structure in the absence and presence of a peptide, it has been shown how a peptide with charge +7 does not reach the threshold concentration necessary to induce membrane disruption. This behavior seems to be associated with the fact that poor insertion into the lipid bilayer cannot screen out the electrostatic repulsion between peptides, and there is mutual repulsion between neighboring peptides, resulting in a low concentration of peptides adsorbed on the lipid bilayer. This behavior contrasts with that obtained for the peptide with charge +4, whose tendency to protrude into the lipid bilayer reduces the electrostatic repulsions between neighboring peptides. This behavior permits a threshold concentration that is sufficient to induce the disruption of the membrane, that is, its lytic activity.

Finally, a thermodynamic study of the peptide insertion into the lipid bilayer points to the entropy being the key property that links the charge/structure of these peptides with their lytic activity.

MODEL AND METHODS

Antimicrobial Peptides. Two different peptides were used as models in the study with primary structures *RQWRRWWQR-NH$_2$* (pep+4) and *RKFRRKFKK-NH$_2$* (pep +7), with charges +4 and +7, respectively. General information about the synthesis of both peptides is given below, and for more details, see refs 30 and 31.

Peptide Synthesis and Antibacterial Activity. The synthesis of both peptides described above was carried out in a solid phase, following the experimental procedure described elsewhere.[30] The microorganism used to determine their antibacterial activity was provided by the laboratorio de Microbiologia, Facultad de Ciencias Medicas, Universidad Nacional de Cuyo, Mendoza, Argentina, Laboratorio de Microbiologia, Hospital Marcial Quiroga, San Juan, Argentina, and Pasteur Institute. Furthermore, the minimal inhibitory concentrations of these peptides were determined using the broth microdilution method following the methodology described elsewhere,[29] in which all the assays were carried out in triplicate.

Cell Membrane Model. A zwitterionic phospholipid bilayer of DPPC composed of 648 DPPC molecules (324 per leaflet) and 28 526 water molecules of the single point charge (SPC)[50] was considered as the cell membrane model in our simulations. The reason for choosing a zwitterionic bilayer for the simulations is based on the previous results obtained for the dynamics action mechanism.[17] This work[17] demonstrated how small cationic peptides induce phospholipid segregations of lipid domains, prior to showing lytic activity, when they reach a threshold concentration on the surface of the cell membrane and then penetrate into the membrane of those domains that are rich in zwitterionic phospholipids.

MD Simulations. GROMACS 4.5.3[51,52] was the package used to carry out the MD simulations. All the simulations were performed in NPT conditions, using the algorithm proposed by Berendsen,[53] with coupling constants of 0.1 and 1 ps for temperature and pressure, respectively. The temperature of all our simulations was 350 K, which is above the transition temperature of 314 K of DPPC bilayers.[38] The long-range interactions were simulated using the Lennard-Jones potential,

DOI: 10.1021/acsomega.8b00293
ACS Omega 2018, 3, 5390−5398

and the electrostatic interactions were calculated using the particle mesh Ewald method[54,55] with a cutoff of 1 nm. The molecular bonds were restrained using LINCS algorithm.[56] The SPC water model[50] was considered in all our simulations.

A trajectory length of 200 ns was simulated in all the cases studied in this work. The force field used in this work was the same as that described in a previous work[17] using the GROMOS 54A7 force field[57] implemented in the GROMACS package.

Molecular Electrostatic Potentials. Quantum mechanics calculations were carried out using the Gaussian 09 program,[58] and the most populated conformations of peptides one and two were obtained from MD simulations. Subsequently, single point density functional theory (DFT) calculations were carried out. Correlation effects were included using DFT with the Becke-3−Lee−Yang−Parr (RB3LYP)[59,60] functional and 6-31++G(d,p) basis set for all the complexes. During the DFT calculations, the geometries were kept fixed. The electronic study was carried out using MEPs.[32] Graphical presentations were created using the MOLEKEL program 2.3.3 MEPs.

AUTHOR INFORMATION

Corresponding Authors

*E-mail: javier.lopez@upct.es (J.J.L.C.).
*E-mail: denriz@unsl.edu.ar (R.D.E.).

ORCID

José Javier López Cascales: 0000-0003-1071-7024

Present Address

#Universidad Politécnica de Cartagena, Grupo de Bioinformatica y Macromoleculas (BioMac), Area de Química Física, Aulario II, Campus de Alfonso XIII, 30203 Cartagena, Murcia, Spain.

Notes

The authors declare no competing financial interest.

ACKNOWLEDGMENTS

The authors acknowledge the financial support from Fundación Séneca through the grant no. 19353/PI/14.

REFERENCES

(1) Jenssen, H.; Hamill, P.; Hancock, R. E. W. Peptide Antimicrobial Agents. *Clin. Microbiol. Rev.* **2006**, *19*, 492−511.
(2) Bulet, P.; Hetru, C.; Dimarcq, J.-L.; Hoffmann, D. Antimicrobial peptides in insects; structure and function. *Dev. Comp. Immunol.* **1999**, *23*, 329−344.
(3) Matsuzaki, K. Why and how are peptide−lipid interactions utilized for self-defense? Magainins and tachyplesins as archetypes. *Biochim. Biophys. Acta* **1999**, *1462*, 1−10.
(4) Hancock, R. E. W.; Diamond, G. The role of cationic antimicrobial peptides in innate host defences. *Trends Microbiol.* **2000**, *8*, 402−410.
(5) Zasloff, M. Antimicrobial peptides of multicellular organisms. *Nature* **2002**, *415*, 389−395.
(6) Guaní-Guerra, E.; Santos-Mendoza, T.; Lugo-Reyes, S.; Terán, L. M. Antimicrobial peptides: General overview and clinical implications in human health and disease. *Clin. Immunol.* **2010**, *135*, 1−11.
(7) LaRock, C. N.; Nizet, V. Cationic antimicrobial peptide resistance mechanisms of streptococcal pathogens. *Biochim. Biophys. Acta* **2015**, *1848*, 3047−3054.
(8) Fernandez, D.; Gehman, J. D.; Separovic, F. Membrane interactions of antimicrobial peptides from Australian frogs. *Biochim. Biophys. Acta* **2009**, *1788*, 1630−1638.
(9) Won, H.-S.; Kang, S.-J.; Lee, B.-J. Action mechanism and structural requirements of the antimicrobial peptides, gaegurins. *Biochim. Biophys. Acta* **2009**, *1788*, 1620−1629.
(10) Harrison, P. L.; Abdel-Rahman, M. A.; Strong, P. N.; Tawfik, M. M.; Miller, K. Characterisation of three α-helical antimicrobial peptides from the venom of scorpio maurus palmatus. *Toxicon* **2016**, *117*, 30−36.
(11) Shai, Y. Mechanism of the binding, insertion and destabilization of phospholipid bilayer membranes by α-helical antimicrobial and cell non-selective membrane-lytic peptides. *Biochim. Biophys. Acta* **1999**, *1462*, 55−70.
(12) Chou, H.-T.; Kuo, T.-Y.; Chiang, J.-C.; Pei, M.-J.; Yang, W.-T.; Yu, H.-C.; Lin, S.-B.; Chen, W.-J. Design and synthesis of cationic antimicrobial peptides with improved activity and selectivity against Vibrio spp. *Int. J. Antimicrob. Agents* **2008**, *32*, 130−138.
(13) Zelezetsky, I.; Tossi, A. α-helical antimicrobial peptides—using a sequence template to guide structure−activity relationship studies. *Biochim. Biophys. Acta* **2006**, *1758*, 1436−1449.
(14) Sitaram, N.; Nagaraj, R. Interaction of antimicrobial peptides with biological and model membranes: structural and charge requirements for activity. *Biochim. Biophys. Acta* **1999**, *1462*, 29−54.
(15) Enriz, R. D.; Suvire, F. D.; Andujar, S. A.; Alvarez, M. A.; Vettorazzi, M.; Dolab, J. G.; Rojas, S. The long and winding road to convert an antimicrobial compound into an antimicrobial drug: An overview from a medicinal chemistry point of view. *Curr. Org. Chem.* **2017**, *21*, 1−11.
(16) Cascales, J. J. L.; Costa, S. D. O.; Garro, A.; Enriz, R. D. Mechanical properties of binary DPPC/DPPS bilayers. *RSC Adv.* **2012**, *2*, 11743−11750.
(17) Cascales, J. J. L.; Garro, A.; Porasso, R. D.; Enriz, R. D. The dynamic action mechanism of small cationic antimicrobial peptides. *Phys. Chem. Chem. Phys.* **2014**, *16*, 21694−21705.
(18) Yeaman, M. R.; Yount, N. Y. Mechanisms of antimicrobial peptide action and resistance. *Pharmacol. Rev.* **2003**, *55*, 27−55.
(19) Epand, R. M.; Vogel, H. J. Diversity of antimicrobial peptides and their mechanisms of action. *Biochim. Biophys. Acta* **1999**, *1462*, 11−28.
(20) Bechinger, B.; Lohner, K. Detergent-like actions of linear amphipathic cationic antimicrobial peptides. *Biochim. Biophys. Acta* **2006**, *1758*, 1529−1539.
(21) Teixeira, V.; Feio, M. J.; Bastos, M. Role of lipids in the interaction of antimicrobial peptides with membranes. *Prog. Lipid Res.* **2012**, *51*, 149−177.
(22) Matsuzaki, K. Control of cell selectivity of antimicrobial peptides. *Biochim. Biophys. Acta* **2009**, *1788*, 1687−1692.
(23) Memariani, H.; Shahbazzadeh, D.; Sabatier, J.-M.; Memariani, M.; Karbalaeimahdi, A.; Bagheri, K. P. Mechanism of action and in vitro short hybrid antimicrobial peptide PV3 against Pseudomonas aeruginosa. *Biochem. Biophys. Res. Commun.* **2016**, *479*, 103−108.
(24) Kim, S. S.; Kim, S.; Kim, E.; Hyun, B.; Kim, K.-K.; Lee, B. J. Synergistic inhibitory effect of cationic peptides and antimicrobial agents on the growth of oral streptococci. *Caries Res.* **2002**, *37*, 425−430.
(25) Marr, A.; Gooderham, W.; Hancock, R. Antibacterial peptides for therapeutic use: obstacles and realistic outlook. *Curr. Opin. Pharmacol.* **2006**, *6*, 468−472.
(26) Gottler, L. M.; Ramamoorthy, A. Structure, membrane orientation, mechanism, and function of pexiganan—A highly potent antimicrobial peptide designed from magainin. *Biochim. Biophys. Acta* **2009**, *1788*, 1680−1686.
(27) Bommarius, B.; Jenssen, H.; Elliott, M.; Kindrachuk, J.; Pasupuleti, M.; Gieren, H.; Jaeger, K.-E.; Hancock, R. E. W.; Kalman, D. Cost-effective expression and purification of antimicrobial and host defense peptides in Escherichia coli. *Peptides* **2010**, *31*, 1957−1965.
(28) Garro, A. D.; Olivella, M. S.; Bombasaro, J. A.; Lima, B.; Tapia, A.; Feresin, G.; Perczel, A.; Somlai, C.; Penke, B.; Cascales, J. L.; et al. Penetratin and derivatives acting as antibacterial agents. *Chem. Biol. Drug Des.* **2013**, *82*, 167−177.

DOI: 10.1021/acsomega.8b00293
ACS Omega 2018, 3, 5390−5398

(29) Parravicini, O.; Somlai, C.; Andujar, S.; Garro, A.; Lima, B.; Tapia, A.; Feresin, G.; Perczel, A.; Toth, G.; Cascales, J.; et al. Small Peptides Derived from Penetratin as Antibacterial Agents. *Arch. Pharm.* **2016**, *349*, 241−251.
(30) Garro, A. D.; Garibotto, F. M.; Rodriguez, A. M.; Raimondi, M.; Zacchino, S. A.; Perczel, A.; Somlai, C.; Penke, B.; Enriz, R. D. New small-size antifungal peptides: Design, synthesis and antifungal activity. *Lett. Drug Des. Discovery* **2011**, *8*, 562−567.
(31) Masman, M. F.; Rodríguez, A. M.; Raimondi, M.; Zacchino, S. A.; Luiten, P. G. M.; Somlai, C.; Kortvelyesi, T.; Penke, P.; Enriz, R. D. Penetratin and derivatives acting as antifungal agents. *Eur. J. Med. Chem.* **2009**, *2*, 212−228.
(32) Polilzer, P.; Truhlar, D. *Chemical Applications of Atomic and Molecular Electrostatic Potentials*; Plenum Publishing: New York, 1991; pp 309−406
(33) Lensink, M. F.; Christiaens, B.; Vandekerckhove, J.; Prochiantz, A.; Rosseneu, M. Penetratin-Membrane Association: W48/R52/W56 Shield the Peptide from the Aqueous Phase. *Biophys. J.* **2005**, *88*, 939−952.
(34) Christiaens, B.; Grooten, J.; Reusens, M.; Joliot, A.; Goethals, M.; Vandekerckhove, J.; Prochiantz, A.; Rosseneu, M. Membrane interaction and cellular internalization of penetratin peptides. *Eur. J. Biochem.* **2004**, *271*, 1187−1197.
(35) Derossi, D.; Joliot, A. H.; Chassaing, G.; Prochiantz, A. The third helix of the Antennapedia homeodomain translocates through biological membranes. *J. Biol. Chem.* **1994**, *269*, 10444−10450.
(36) Lindberg, M.; Biverståhl, H.; Gräslund, A.; Mäler, L. Structure and positioning comparison of two variants of penetratin in two different membrane mimicking systems by NMR. *Eur. J. Biochem.* **2003**, *270*, 3055−3063.
(37) Letoha, T.; Gaál, S.; Somlai, C.; Venkei, Z.; Glavinas, H.; Kusz, E.; Duda, E.; Czajlik, A.; Peták, F.; Penke, B. Investigation of penetratin peptides. Part 2. In vitro uptake of penetratin and two of its derivatives. *J. Pept. Sci.* **2005**, *11*, 805−811.
(38) Seelig, A.; Seelig, J. Dynamic structure of fatty acyl chains in a phospholipid bilayer measured by deuterium magnetic resonance. *Biochemistry* **1974**, *23*, 4839−4845.
(39) López Cascales, J. J.; de la Torre, J. G.; Marrink, S. J.; Berendsen, H. J. C. Molecular dynamics simulation of a charged biological membrane. *J. Chem. Phys.* **1996**, *104*, 2713−2720.
(40) Brown, M. F. Theory of spin-lattice relaxation in lipid bilayers and biological membranes. ^{2}H and ^{14}N quadrupolar relaxation. *J. Phys. Chem.* **1982**, *77*, 1576−1599.
(41) Evans, E.; Rawicz, W. Entropy-driven tension and bending elasticity in condensed-fluid membranes. *Phys. Rev. Lett.* **1990**, *64*, 2094−2097.
(42) Rawicz, W.; Olbrich, K. C.; McIntosh, T.; Needham, D.; Evans, E. Effect of chain length and unsaturation on elasticity of lipid bilayers. *Biophys. J.* **2000**, *79*, 328−339.
(43) Seto, H.; Yamada, N. L.; Nagao, M.; Hishida, M.; Takeda, T. Bending modulus of lipid bilayers in a liquid-crystalline phase including an anomalous swelling regime estimated by neutron spin echo experiments. *Eur. Phys. J. E* **2008**, *26*, 217−223.
(44) Lindahl, E.; Edholm, O. Spatial and energetic-entropic decomposition of surface tension in lipid bilayers from molecular dynamics simulations. *J. Chem. Phys.* **2000**, *113*, 3882−3893.
(45) Kamo, T.; Nakano, M.; Kuroda, Y.; Handa, T. Effects of an Amphipathic α-Helical peptide on lateral pressure and water penetration in phosphatidylcholine and monoolein mixed membranes. *J. Phys. Chem. B* **2006**, *49*, 24987−24992.
(46) Torrie, G. M.; Valleau, J. P. Nonphysical sampling distributions in Monte Carlo free-energy estimation: Umbrella Sampling. *J. Comput. Phys.* **1977**, *23*, 187−199.
(47) Kumar, S.; Rosenberg, J. M.; Bouzida, D.; Swendsen, R. H.; Kollman, P. A. The weighted histogram analysis method for free-energy calculations on biomolecules. I. The method. *J. Comput. Chem.* **1992**, *13*, 1011−1021.
(48) Gottler, L. M.; Lee, H.-Y.; Shelburne, C. E.; Ramamoorthy, A.; Marsh, E. N. G. Using fluorous amino acids to modulate the biological activity of an antimicrobial peptide. *ChemBioChem* **2008**, *9*, 370−373.
(49) Wenk, M. R.; Seelig, J. Magainin 2 amide interaction with lipid membranes: calorimetric detection of peptide binding and pore formation. *Biochemistry* **1998**, *37*, 3909−3916.
(50) Berendsen, H. J. C.; Postma, J. P. M.; van Gunsteren, W. F.; Hermans, J. Interaction models for water in relation to protein hydration. *Intermolecular Forces*; Pullman, B., Ed.; D. Reidel Publishing Company, 1981; Vol. *1*, pp 331−342
(51) Berendsen, H. J. C.; van der Spoel, D. V.; van Drunen, R. GROMACS—a message-passing parallel molecular dynamics implementation. *Comput. Phys. Commun.* **1995**, *91*, 43−56.
(52) Lindahl, E.; Hess, B.; van der Spoel, D. GROMACS 3.0: a package for molecular simulation and trajectory analysis. *J. Mol. Model.* **2001**, *7*, 306−317.
(53) Berendsen, H. J. C.; Postma, J. P. M.; van Gunsteren, W. F.; DiNola, A.; Haak, J. R. Molecular dynamics with coupling to an external bath. *J. Chem. Phys.* **1984**, *81*, 3684−3690.
(54) Darden, T.; York, D.; Pedersen, L. Particle mesh Ewald: an N log(N) method for Ewald sums in large systems. *J. Chem. Phys.* **1993**, *98*, 10089−10092.
(55) Essmann, U.; Perera, L.; Berkowitz, M. L.; Darden, T.; Lee, H.; Pedersen, L. G. A smooth particle mesh Ewald method. *J. Chem. Phys.* **1995**, *103*, 8577−8593.
(56) Hess, B.; Bekker, H.; Berendsen, H. J. C.; Fraaije, J. G. E. M. LINCS: a linear constraint solver for molecular simulations. *J. Comput. Chem.* **1997**, *18*, 1463−1472.
(57) Schmid, N.; Eichenberger, A. P.; Choutko, A.; Riniker, S.; Winger, M.; Mark, A. E.; van Gunsteren, W. F. Definition and testing of the GROMOS force-field versions 54A7 and 54B7. *Eur. Biophys. J.* **2011**, *7*, 843−856.
(58) Frisch, M. J.; Trucks, G.; Schlegel, H.; Robb, G. S.; Cheeseman, J.; Montgomery, J.; Vreven, T.; Kudin, K.; Burant, J.; Millam, J.; et al. *Gaussian 03*, Revision B.03; Gaussian, Inc.: Pittsburgh, PA, 2003.
(59) Becke, A. D. Density-functional exchange-energy approximation with correct asymptotic behavior. *Phys. Rev. A: At., Mol., Opt. Phys.* **1988**, *38*, 3098−3100.
(60) Becke, A. D. Density-functional thermochemistry. III. The role of exact exchange. *J. Chem. Phys.* **1993**, *98*, 5648.

DOI: 10.1021/acsomega.8b00293
ACS Omega 2018, 3, 5390−5398